

Late time dynamics of scalar perturbations outside black holes.

II. Schwarzschild geometry

Leor Barack*

Department of Physics, Technion—Israel Institute of Technology, Haifa, 32000, Israel

(February 7, 2008)

We apply a new analytic scheme, developed in a preceding paper, in order to calculate the late time behavior of scalar test fields evolving outside a Schwarzschild black hole. The pattern of the late time decay at future null infinity is found to be the same as in the shell toy-model studied in the preceding paper. A simple late time expansion of the scalar field is then used, relying on the results at null infinity, to construct a complete picture of the late time wave behavior anywhere outside the black hole. This reproduces the well known power-law tails at time-like infinity and along the event horizon. The main motivation for the introduction of the new approach arises from its applicability to rotating black holes, as shall be discussed in a forthcoming paper.

04.70.Bw, 04.25.Nx

I. INTRODUCTION

It is well established that the gravitational field of a generically forming black holes relaxes at late time to a “no-hair” stationary Kerr-Newman geometry. It was first demonstrated by Price [1], regarding gravitational and electro-magnetic perturbations of the Schwarzschild black hole (SBH) exterior, that the fields die off at late time with an inverse power-law tail. For a spherical-harmonic wave mode of multipole number l , it was shown that a $t^{-(2l+2+p)}$ decay tail (t being the Schwarzschild time coordinate) will be detected by a static observer outside the black hole, with $p = 1$ if an initially compact perturbation is considered, or $p = 0$ in case that a static field existed outside the central object before the onset of collapse.

These results were later confirmed using several different techniques, both analytic and numerical [2–5], and were generalized to other spherically-symmetric spacetimes [2,6,7]. The application of perturbative (linear) approaches is encouraged by numerical analysis of the fully non-linear dynamics of the fields [7,8], which indicates virtually the same late time pattern of decay, as for the minimally-coupled (linear) fields.

Power-law decay tails are exhibited by fields at late time, because in a curved spacetime waves do not propagate merely along light cones, even when the fields are massless. Rather, the waves spread inside the light cones due to scattering off spacetime curvature. As suggested by previous studies, the late time behavior of these waves is characteristic of merely the large distance structure of spacetime. This implies that the phenomenon of late time tails may not necessarily be restricted to the exteriors of black holes. For example, late time tails are found to form during the purely spherical collapse of a self-gravitating minimally coupled scalar field, even when the collapse fails to create a black hole [8]. Conversely, no power law tails are detected in the non-asymptotically-

flat geometries of Schwarzschild–de Sitter and Reissner–Nordström–de Sitter black holes [9] (instead, the field is found to die off exponentially at late time in these cases).

All previously mentioned studies were benefited from the simplicity of spherical symmetry. Yet, an astrophysically realistic model should clearly employ a rotating central object. Thus, apparently the most tempting generalization of the analysis involves the inclusion of angular momentum in the background geometry. A first progress in this direction has been achieved recently with the introduction of a full (1+2 dimensions) numerical analysis of wave dynamics in Kerr spacetime, by Krivan *et al.* [10,11]. So far, however, no *analytic* scheme has been proposed for the investigation of wave dynamics in Kerr.

In a preceding paper (to be referred to as **paper I**) we introduced an analytic technique for the study of late time behavior of fields in asymptotically-flat spacetimes. The prime motivation for the introduction of the new scheme was its applicability to rotating black holes. To examine the essential features of the proposed calculation scheme, we applied it in paper I to study the simple toy-model of a scalar field evolving outside a spherically-symmetric thin shell of matter. In that case, the new technique, based on what we called “*the iterative expansion*”, allowed a simple and rigorous derivation of the late time waves-form at null infinity. In the present paper we apply a variant of the iterative scheme in order to analyze the evolution of scalar waves on the background of the *complete Schwarzschild geometry*. Again, this method will enable the analytic calculation of the late time behavior at null infinity. We shall then show how, relying on the results at null infinity, it becomes rather simple to construct a complete picture of the late time decay anywhere outside the black hole, in particular along the event horizon.

There are several reasons why we think it is worthwhile to first analyze the already well-studied case of a SBH, rather than directly focus on the more interesting case

of the Kerr black hole. First, this will enable us to test our scheme against the well-established results available in the Schwarzschild case. Secondly, many parts of the analysis in Schwarzschild shall later be directly employed when analyzing scalar waves in Kerr [12,13]. Finally, the analysis in Schwarzschild will appear to be valuable on its own right, providing, in some respects, a more complete picture of the late-time wave behavior than already available.

In the shell model, spacetime is flat at small distances (inside the shell). For that reason, the complete internal geometry could be exactly accounted for by merely the “Minkowski-like” first component of the iterative expansion (denoted in paper I by Ψ_0). (we remind that the terms $\Psi_{N \geq 1}$ of the iterative expansion were describing deviations from flat geometry, namely curvature effects outside the shell.) The complete Schwarzschild manifold, however, does not share this convenient property, as in this case spacetime is highly curved at small distances. This will enforce us to choose for another “basis” potential for the iterative scheme at small r (other than the purely-centrifugal potential V_0 chosen in the framework of the shell model), and will thus somewhat complicate the technical details of the analysis. Nevertheless, the basic calculation scheme, as well as the results at null infinity, shall remain essentially the same as in the shell model.

arrangement of this paper

This paper is arranged as follows. In sec. II we give a mathematical formulation of the wave evolution problem in Schwarzschild as a characteristic two-dimensional initial-value problem. In sec. III we introduce the iterative scheme to be used to allow an analytic treatment of the mathematical problem. We apply the iterative calculation scheme in sections IV through VII, obtaining an expression for the waves-form at late time at null infinity. Then, in sec. VIII, a simple technique is applied to obtain the late time behavior of the scalar field at any constant r (including along the event horizon). Sec. IX summarizes the results and discusses possible extensions of the analysis.

II. THE INITIAL VALUE PROBLEM

We consider the evolution of initial data, representing a generic pulse of massless scalar radiation, on a fixed SBH background. The scalar field is assumed to satisfy the (minimally-coupled) Klein–Gordon equation

$$\Phi_{;\mu}^{\;\mu} = 0, \quad (1)$$

where Φ represents the scalar wave. The structure of spacetime affects the evolution of the scalar field through

the covariant derivatives, denoted in Eq. (1) by semi-colons.

Decomposing the field into spherical harmonics,

$$\Phi(t, r, \theta, \varphi) = \sum_{l=0}^{\infty} \sum_{m=-l}^l \phi^l(t, r) Y_{lm}(\theta, \varphi), \quad (2)$$

we obtain an independent equation for each of the components $\phi^l(t, r)$,

$$f^{-1}(r)\phi_{,tt}^l - f(r)\phi_{,rr}^l - \frac{2(r-M)}{r^2}\phi_{,r}^l + \frac{l(l+1)}{r^2}\phi^l = 0. \quad (3)$$

Here t , r , θ and φ are the standard Schwarzschild coordinates, M is the mass of the black hole, $f(r) \equiv (1-2M/r)$, and l is the multipole number of the mode under consideration.

A more convenient form for the wave equation may be obtained in terms of a new wave function $\Psi^l(t, r) \equiv r\phi^l(t, r)$. To that end we introduce the double-null (Eddington–Finkelstein) coordinates $v \equiv t + r_*$ and $u \equiv t - r_*$, where

$$r_* = r + 2M \ln \left(\frac{r - 2M}{2M} \right). \quad (4)$$

The “tortoise” coordinate r_* varies monotonically from $-\infty$ (the event horizon) to $+\infty$ (space-like infinity).

The wave equation now reads

$$\Psi_{,uv}^l + V^l(r)\Psi^l = 0, \quad (5)$$

in which

$$V^l(r) = \frac{1}{4} \left(1 - \frac{2M}{r} \right) \left[\frac{l(l+1)}{r^2} + \frac{2M}{r^3} \right] \quad (6)$$

is an effective potential, accounting for both centrifugal and curvature effects. This effective potential is sketched in figure 1 as a function of r_* for the sample values $l = 0, 1, 2$.

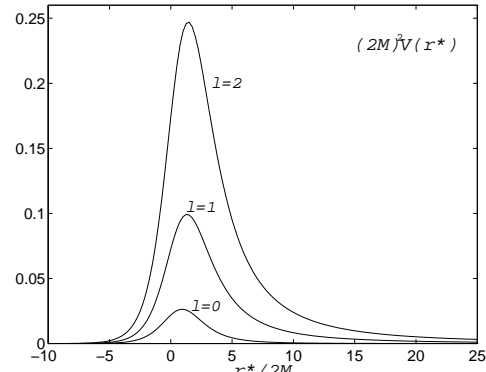


FIG. 1. Effective potential for scalar waves in Schwarzschild spacetime. With r_* defined as in Eq. (4), we have $r_* = 0$ corresponding to $r \simeq 2.56M$.

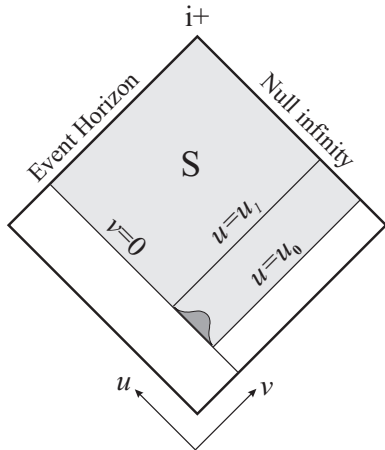
Note the following features of the effective potential (valid for all values of l), which play an important role in our analysis. $V(r)$ is *localized* (in a sense apparent in figure 1), forming an effective potential barrier for the waves. At large distance, $V(r)$ is dominated by the centrifugal potential (reflecting asymptotic flatness), with curvature-induced deviations which die off as $\sim r^{-3}$. At small r_* values, $V(r)$ dies off exponentially in r_*/M towards the event horizon, making the potential effectively zero inside the potential barrier. Evidently, the late time behavior at null infinity is affected mostly by the shape of the potential at large distance. Conversely, the early evolution (e. g. the quasinormal ringing stage), is strongly related to the fine details of the potential shape at small r values.

Since each of the spherical harmonics modes evolves separately, we henceforth discuss the evolution of a single mode of arbitrary multipole number l . The superscript ' l ' (denoting l -dependence) will usually be suppressed for brevity.

The initial data for the evolution problem shall be specified on two characteristic (null) surfaces outside the event horizon, as sketched in the Penrose diagram of figure 2. We will first consider initial data in the form of some compact outgoing pulse, specified on the ingoing null surface $v = 0^*$,

$$\begin{cases} \Psi(u = u_0) = 0 \\ \Psi(v = 0) = \Gamma(u) \end{cases}, \quad (7)$$

where $\Gamma(u)$ is some function of a compact support ("the pulse") between retarded times $u = u_0$ and $u = u_1$. As demonstrated in paper I for the shell model, the case of static initial field can be later inferred in a simple way from the result regarding a compact pulse.



*As long as u_0 remains a free parameter in the analysis, the specific choice $v = 0$ causes no loss of generality, since spacetime is time-translation invariant.

FIG. 2. The set-up of initial data. Shown is the Penrose diagram representing the external Schwarzschild geometry. The dark feature (artificially shown as if extended to $v > 0$ values) represents the amplitude of some compact support initial function $\Gamma(u)$ on the ray $v = 0$. The initial problem for the scalar field is well posed in region S (the shadowed area).

The evolution equation (5), supplemented by the initial conditions (7), establishes a well posed characteristic initial value problem for the scalar field anywhere in the domain S outside the event horizon (see figure 2). Since, manifestly, this problem poses no mathematical irregularities, existence and uniqueness of a solution are guaranteed by fundamental mathematical theory (see, for example, [14]).

III. THE ITERATIVE EXPANSION

To define the iterative expansion to be applied in the complete SBH model, we first introduce a new parameter, $r_0 > 0$, its value chosen so that $r(r_* = r_0)$ is of order $\gtrsim 2M$ [say, $r(r_* = r_0) = 3M$]. We then define

$$V_0(r_*) \equiv \begin{cases} 0 & , r_* < r_0 \\ \frac{l(l+1)}{4r_*^2} & , r_* \geq r_0 \end{cases} \quad (8)$$

and

$$\delta V(r) \equiv V - V_0, \quad (9)$$

in which $V(r)$ is the Schwarzschild effective potential given by Eq. (6). The potential $V_0(r_*)$ is so defined to account for the fact that the actual effective potential is exponentially small at small r_* values. With this definition, the function $V_0(r_*)$ approximates the form of the actual effective potential $V(r_*)$ at both the very large and the very small values of r_* (The deviations, described by δV , become significant only at intermediate distances, see figure 1).

Following the same procedure as in studying the shell model, we define the *iterative expansion* by decomposing the scalar wave Ψ into an infinite sum,

$$\Psi = \sum_{N=0}^{\infty} \Psi_N, \quad (10)$$

in which the components Ψ_N are defined in a recursive way by the hierarchy of equations

$$\Psi_{N,uv} + V_0 \Psi_N = \begin{cases} 0 & , N = 0 \\ -(\delta V) \Psi_{N-1} & , N > 0 \end{cases}, \quad (11)$$

supplemented by the initial data

$$\Psi_N(u = u_0) = 0 \quad (\forall N \geq 0), \quad (12a)$$

$$\Psi_N(v = 0) = \begin{cases} \Gamma(u) & , N = 0 \\ 0 & , N > 0 \end{cases}. \quad (12b)$$

Formal summation over N recovers the “complete” initial value problem for the scalar wave Ψ .

It was indicated in paper I that in the analogous shell model the iterative sum seems to converge rather efficiently at late time to the actual field at null infinity, provided that the initial pulse is specified at large distance. In that case, it was suggested both numerically and analytically that the “complete” wave is well approximated by merely the function Ψ_1 . With this result in mind, we are going, in the following, to derive exact analytic expressions for Ψ_0 and for the (time domain) Green’s function in the complete SBH model. We shall then use these results to calculate the late time form of Ψ_1 at null infinity in this model.

The above iterative expansion appears to be an effective calculation scheme for all modes l of the scalar radiation, except for the monopole mode $l = 0$. This is unlike the scheme used for the shell model in paper I, which held equally-well for all modes l with no exception. The reason for this difference between the two models in the monopole case will be discussed later. The calculation to follow shall regard only the modes with $l > 0$.

IV. DERIVATION OF Ψ_0

We first obtain an explicit expression for Ψ_0 , the first element of the iterative expansion. Since the only discontinuity in the potential function V_0 (at $r_* = r_0$) is bounded in magnitude, we learn by the wave equation (11) that Ψ_0 and its first order derivatives should be continuous anywhere. In the sequel we explicitly use this fact in constructing an expression for Ψ_0 .

We shall consider separately three distinct regions of the domain S , as indicated in figure 3. Regions I ($u_0 < u < -2r_0$) and II ($u > -2r_0, r_* > r_0$) cover the part of S outside the surface $r_* = r_0$, while region III ($r_* < r_0$) is the portion inside this surface.

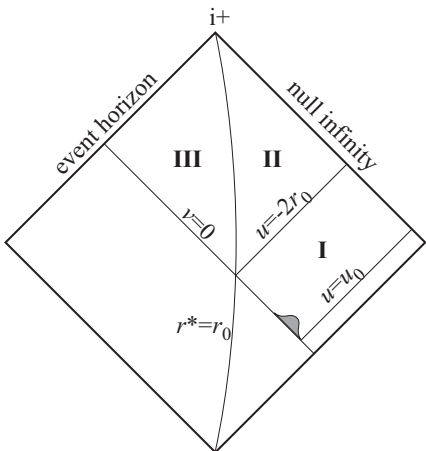


FIG. 3. Calculation of Ψ_0 in the complete Schwarzschild geometry. The solution in each of the regions labeled I, II, and III is discussed separately in the text.

A solution to Eq. (11) for $N = 0$ has the general form[†]

$$\Psi_{0I} = \sum_{n=0}^l A_n^l \frac{g_{0I}^{(n)}(u)}{(v-u)^{l-n}} \quad (13a)$$

$$\Psi_{0II} = \sum_{n=0}^l A_n^l \frac{g_{0II}^{(n)}(u)}{(v-u)^{l-n}} \quad (13b)$$

$$\Psi_{0III} = F(u) + H(v), \quad (13c)$$

in which the labels I, II, III denote the region to which each specific solution corresponds, and where $g_{0I}(u)$, $g_{0II}(u)$, $F(u)$ and $H(v)$ are (yet) arbitrary functions. In the above equations the coefficients A_n^l are given by

$$A_n^l = \frac{(2l-n)!}{n!(l-n)!}, \quad (14)$$

and the parenthetical indices indicate the number of times the functions are differentiated.

Causality implies that in region I, the solution $\Psi_{0I}(u)$ cannot be sensitive to the form of V_0 at $r_* < r_0$. Thus it must be identical to the solution derived in the shell model, with the function $g_{0I}(u)$ explicitly related to the initial data function by

$$g_{0I}(u) = \frac{1}{(l-1)!} \int_{u_0}^u \left(\frac{u}{u'} \right)^{l-1} (u-u')^{l-1} \Gamma(u') du' \quad (15)$$

(see paper I for details).

Now, with the initial condition $\Psi_{0III}(v=0) = 0$ [‡], Eq. (13c) implies that Ψ_{0III}^{III} is a function of v only. We can then use the continuity of Ψ_{0III} at $r_* = r_0$ to derive a closed differential equation for the function $g_{0II}(u)$:

$$\frac{\partial}{\partial u} \left\{ \sum_{n=0}^l A_n^l \frac{[g_{0II}(u)]^{(n)}}{(v-u)^{l-n}} \right\} \Big|_{r_* = r_0} = 0. \quad (16)$$

This equation may be put into the form

$$\sum_{n=0}^{l+1} B_n^l r_0^n [g_{0II}(u)]^{(n)} = 0, \quad (17)$$

in which the coefficient B_n^l are given by

[†] The most general solution at $r > r_0$ involves also an arbitrary function $h(v)$. However, for our choice of initial setup (an outgoing initial pulse), the solution Ψ_0 can be expressed in terms of a function $g(u)$ solely. This issue is discussed in appendix A of paper I.

[‡] Since we shall be interested mostly in the case where the initial pulse is specified at large distance, we assume here that its support is confined to the exterior of the sphere $r_* = r_0$.

$$B_n^l = \frac{2^n(2l-n)!}{n!(l-n+1)!}. \quad (18)$$

Thus $g_{0II}(u)$ is a solution of a constant-coefficients linear equation of order $l+1$. It therefore admits the form

$$g_{0II}(u) = \sum_{i=1}^{l+1} C_i \exp(-\kappa_i u/r_0), \quad (19)$$

where C_i are constants, and the $l+1$ complex numbers κ_i are the roots of the algebraic equation

$$\sum_{n=0}^{l+1} B_n^l (-\kappa)^n = 0. \quad (20)$$

The only properties of the numbers κ_i important for our discussion are that (i) these numbers are all distinct (for any given value of l), and that (ii) we have $\text{Re}(\kappa_i) > 0$ for all values of l and i . Hence g_0 (and also Ψ_0 itself) falls off exponentially at late retarded time u .

The coefficients C_i are determined by imposing continuity on Ψ_0 at $u = -2r_0$, namely by requiring $(g_{0II})^{(j)} = (g_{0I})^{(j)}$ at $u = -2r_0$, for all $0 \leq j \leq l$. This leads to a set of $l+1$ algebraic equations for the $l+1$ coefficients C_i , having the form

$$\sum_{i=1}^{l+1} M_{ji} C_i = r_0^j g_{0I}^{(j)} \Big|_{u=-2r_0} \quad (21)$$

for $0 \leq j \leq l$, where $M_{ji} \equiv (-\kappa_i)^j \exp(2\kappa_i)$. In a matrix form, we have

$$\det \mathbf{M} = \exp[2(\kappa_1 + \dots + \kappa_{l+1})] \det \mathbf{K}, \quad (22)$$

where \mathbf{K} is the Vandermonde matrix

$$\mathbf{K} = \begin{pmatrix} 1 & 1 & \dots & 1 \\ -\kappa_1 & -\kappa_2 & \dots & -\kappa_{l+1} \\ \vdots & \vdots & & \vdots \\ -\kappa_1^l & -\kappa_2^l & \dots & -\kappa_{l+1}^l \end{pmatrix}, \quad (23)$$

which is always non-singular, provided only that the numbers κ_i are all distinct (which is the case here). Therefore the set of equations (21) has a unique solution for the coefficients C_i .

We finally obtain Ψ_{0II} by substituting for g_{0II} in Eq. (13b). This yields an expression of the form

$$\Psi_{0II} = r_*^{-l} \sum_{n=0}^l \sum_{i=1}^{l+1} \alpha_{ni} \left(\frac{r_*}{r_0} \right)^n E_i(u), \quad (24)$$

in which α_{ni} are constant coefficients (being certain l -dependent functionals of the initial-data function $\Gamma(u)$), and where the functions

$$E_i(x) \equiv \exp[-\kappa_i x/r_0] \quad (25)$$

die off exponentially with respect to their argument for all $1 \leq i \leq l+1$.[§] We still have to derive an expression for Ψ_0 in region III, that is at $r_* < r_0$. By the continuity of Ψ_0 at $r_* = r_0$ we have $\Psi_0^{III}(v) = \Psi_0^{II}(u=v-2r_0)$. It follows that

$$\Psi_0^{III} = r_0^{-l} \sum_{i=1}^{l+1} \alpha_i E_i(v-2r_0), \quad (26)$$

where $\alpha_i \equiv \sum_{n=0}^l \alpha_{ni}$, and where the functions E_i are those defined in Eq. (25).

We conclude that Ψ_0 “penetrates” the potential barrier only through a narrow null ray of typical width $\sim 2r_0$ adjacent to the initial ingoing ray $v=0$. It has significant amplitude only in a “main” region $u_0 < u \lesssim 0$ and along that penetrating null ray. Elsewhere, Ψ_0 is found to be exponentially small (in retarded time u at $r_* > r_0$ or in advanced time v at $r_* < r_0$). This result (valid for all $l \geq 1$) is illustrated in figure 4.

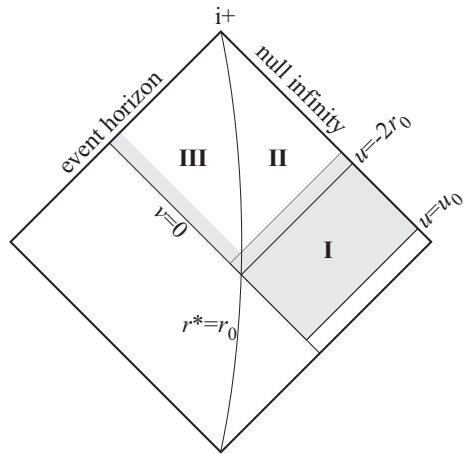


FIG. 4. Domain of the function Ψ_0 in Schwarzschild. Dark colored areas indicate regions where Ψ_0 is not exponentially small. Note that Ψ_0 “penetrates” the potential barrier only through a narrow ingoing ray (of typical width $\sim 2r_0$).

V. CONSTRUCTION OF THE GREEN'S FUNCTION

In this section we derive an analytic expression for the (retarded) Green's function corresponding to the operator $\partial_u \partial_v + V_0(r_*)$, with $V_0(r)$ defined in Eq. (8). The (retarded) Green's function $G(u, v; u', v')$ is defined by the equation

[§] In Eq. (24), as well as in all other expressions for the various functions Ψ to be appeared in this paper, it is to be understand that only the *real* (or alternatively—the *imaginary*) part is taken into account. The indication “Re” shall be omitted for brevity.

$$G_{,uv} + V_0 G = \delta(u - u')\delta(v - v'), \quad (27)$$

supplemented by the causality condition $G(v < v') = G(u < u') = 0$, where (u', v') are the null coordinates of a scalar ‘‘point’’ source (in the 1+1 dimensions representation), and (u, v) is where we evaluate the field this source induces. [It will become evident by construction that this condition specifies a unique solution to Eq. (27).] In view of the results obtained for Ψ_0 , we shall have to consider both ‘‘external’’ ($r'_* > r_0$) and ‘‘internal’’ ($r'_* < r_0$) sources. In what follows we treat each of these two cases separately.

A. External sources

We first consider a ‘‘point’’ source located at null coordinates (u', v') outside the surface $r_* = r_0$ (thus $v' - u' > 2r_0$). For this fixed source, we look for the Green’s function at any evaluation point (u, v) . To that end we separate the future light cone of the point source into three regions, as indicated in figure 5. Regions I and II correspond to evaluation points outside the surface $r_* = r_0$, while region III corresponds to internal evaluation points.

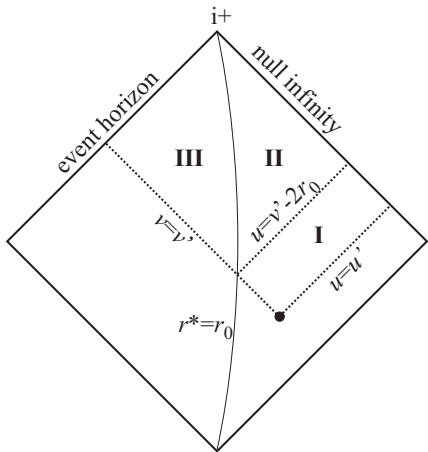


FIG. 5. Construction of the Green’s function for a scalar source sphere at $r'_* > r_0$. The three regions I, II, III, defined with respect to that source, are treated separately in the text.

We first observe that in Region I (that is at $u < v' - 2r_0$) the Green’s function cannot depend on the form of the potential at $r_* < r_0$ (as implied by causality), and thus in this region it must be the same as in the shell model (outside the shell). Therefore, by Eqs. (33) and (35) of paper I we find that the Green’s function in region I reads

$$G^I(u, v; u', v') = \sum_{n=0}^l A_n^l \frac{[g_G^I(u; u', v')]^{(n)}}{(v - u)^{l-n}}, \quad (28)$$

in which the differentiation is with respect to u , A_n^l are the coefficients given in Eq. (14), and

$$g_G^I(u; u', v') = \frac{1}{l!} \left[\frac{(v' - u)(u - u')}{(v' - u')} \right]^l. \quad (29)$$

Now, in regions II and III Eq. (27) is homogeneous, hence the solutions for the Green’s function in these two regions are of the form

$$G^{II} = \sum_{n=0}^l A_n^l \frac{[g_G^{II}(u)]^{(n)}}{(v - u)^{l-n}} \quad (30a)$$

$$G^{III} = G^{III}(v), \quad (30b)$$

where the functions $g^{II}(u)$ and $G^{III}(v)$ are yet to be determined.

By analogy with Eq. (19) we then have

$$g_G^{II}(u) = \sum_{i=1}^{l+1} \bar{C}_i(u', v') \exp(-\kappa_i u / r_0), \quad (31)$$

with κ_i being the same numbers as in Eq. (19), and where the $l+1$ coefficients $\bar{C}_i(u', v')$ are to be determined such that the Green’s function is continuous along the ray $u = v' - 2r_0$. This requirement leads to a set of $l+1$ equations for the coefficients $\bar{C}_i(u', v')$, reading

$$\sum_{i=1}^{l+1} \bar{M}_{ji} \bar{C}_i = r_0^j [g_G^I(u)]^{(j)} \Big|_{u=v'-2r_0} \quad (32)$$

(for $0 \leq j \leq l$), where $\bar{M}_{ji} \equiv (-\kappa_i)^j \exp[-\kappa_i(v' - 2r_0)/r_0]$. The solution (which always exists) is

$$\bar{C}_i = \exp[\kappa_i(v' - 2r_0)/r_0] \sum_{j=0}^l K_{ij}^{-1} r_0^j [g_G^I(u)]^{(j)} \Big|_{u=v'-2r_0}, \quad (33)$$

with K_{ij}^{-1} being the elements of the matrix reciprocal to the Vandermonde matrix (23). Inserting the explicit expression for g_G^I and using Eq. (30a), we can finally obtain for the Green’s function in region II,

$$G^{II} = \sum_{n,j=0}^l \sum_{i=1}^{l+1} \beta_{nji} \frac{(r'_* - r_0)^{l-j} (r_0)^{l+j-n}}{(r'_*)^l r_*^{l-n}} E_i(u - v' + 2r_0), \quad (34)$$

in which $r'_* \equiv (v' - u')/2$, and where β_{nji} are certain constant coefficients (depending on l only). (Recall that the functions E_i die off exponentially with respect to their argument for all i .)

To obtain the Green’s function in region III, we simply notice that $G^{III}(v) = G^{II}(u = v - 2r_0)$, implied by the continuity of G at $r_* = r_0$. It follows that

$$G^{III} = \sum_{j=0}^l \sum_{i=1}^{l+1} \beta_{ji} \frac{(r'_* - r_0)^{l-j} (r_0)^j}{(r'_*)^l} E_i(v - v'), \quad (35)$$

where $\beta_{ji} \equiv \sum_{n=0}^l \beta_{nji}$. (It is straightforward to verify that with this result, we have $G^{III}(v = v') = 1$ as necessary.)

B. Internal sources

To obtain the Green's function for a source point located at $r'_* < r_0$, we refer to figure 6, where again we indicate three regions, defined with respect to a given source at (u', v') . Again we discuss the construction of the Green's function in each of these regions in separate.

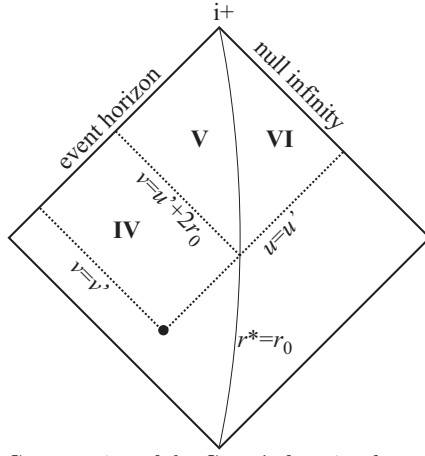


FIG. 6. Construction of the Green's function for a scalar source sphere at $r'_* < r_0$. The three regions IV, V, VI are treated separately in the text.

In region IV we have $G_{,uv}^{IV} = \delta(v - v')\delta(u - u')$ by definition, which (by causality) leads to

$$G^{IV} = \theta(v - v')\theta(u - u'), \quad (36)$$

with θ denoting the usual step function.

In region V the Green's function satisfies the homogeneous equation $G_{,uv}^V = 0$. With the continuity requirement $G^V(v = u' + 2r_0) = 1$, this means that $G^V = G^V(v)$. Now, G^{VI} is given in terms of a function $g_G^{VI}(u)$, in a way analogous to G^{II} in Eq. (30a). By the continuity of $G_{,u}$ at $r'_* = r_0$ we must have $G_{,u}^{VI}(r_* = r_0) = 0$, which is a linear differential equation of order $l + 1$ for the function $g_G^{VI}(u)$. The solution is (in analogy to Eq. (31)),

$$g_G^{VI}(u) = \sum_{i=1}^{l+1} \tilde{C}_i(u', v') \exp[-\kappa_i u / r_0], \quad (37)$$

with \tilde{C}_i being certain coefficients.

To construct the coefficients \tilde{C}_i , we match the function G^{VI} , as inferred by Eq. (37), to its value on the ray $u = u'$. This value may be deduced independently by inserting the form $G^{IV}(u, v) = \bar{G}^{IV}(u, v)\theta(u - u')$ (implied by causality) into equation (27), and observing that a solution must admit $\bar{G}_{,v} = 0$ along $u = u'$. This means that G is constant along this ray. By Eq. (36) (and requiring continuity) we then learn that this constant is unity. Requiring $G^{VI}(u = u') = 1$ for all v then leads to

$$\begin{cases} [g_G^{IV}]^{(n)}(u') = 0 & , \quad (0 \leq n \leq l - 1) \\ [g_G^{IV}]^{(l)}(u') = 1 \end{cases} \quad (38)$$

With Eq. (37), this constructs a set of $l + 1$ linear algebraic equations for the coefficients \tilde{C}_i . The solution reads

$$\tilde{C}_i = r_0^l K_{i,l+1}^{-1} \exp[\kappa_i u' / r_0], \quad (39)$$

where the numbers κ_i are the same as for the external source. (Recall that the matrix \mathbf{K} is always non-singular, hence this solution exist and is unique.)

Using the results (37) and (39) we can finally obtain

$$G^{VI} = \sum_{n=0}^l \sum_{i=1}^{l+1} \gamma_{ni} \left(\frac{r_0}{r_*} \right)^{l-n} E_i(u - u'), \quad (40)$$

with the functions E_i defined in Eq. (25), and where γ_{ni} are certain constant coefficients (depending only on l).

To obtain G^V , we simply notice that $G^V(v) = G^{VI}(u = v - 2r_0)$ (inferred by the continuity of the Green's function), hence

$$G^V = \sum_{i=1}^{l+1} \gamma_i E_i(v - u' - 2r_0), \quad (41)$$

$$\text{where } \gamma_i \equiv \sum_{n=0}^l \gamma_{ni}.$$

C. Fixed external evaluation point

Thus far we considered the Green's function for a given sources at (u', v') , as a function of the evaluation coordinates (u, v) . In practice, we shall be interested in calculating the function Ψ_1 at a given location (specifically—at null infinity, for $u \gg M$), what will involve integration over all possible sources. This requires knowledge of the form of the Green's function at the evaluation location, as a function of the sources locations. To that end we only need to re-interpret our previous results: The expressions we have derived for the Green's function shall be regarded as functions of the source coordinates (u', v') , with fixed evaluation coordinates (u, v) . This reversed presentation of the results is illustrated in figure 7. Indicated in this figure are the regions of spacetime in which scalar sources influence the behavior of the scalar field at a fixed evaluation point (with null coordinates u, v) outside the surface $r_* = r_0$. Dark-colored areas in this figure indicate source regions where the Green's function is *not* exponentially-small, as inferred by Eqs. (28), (34) and (40).

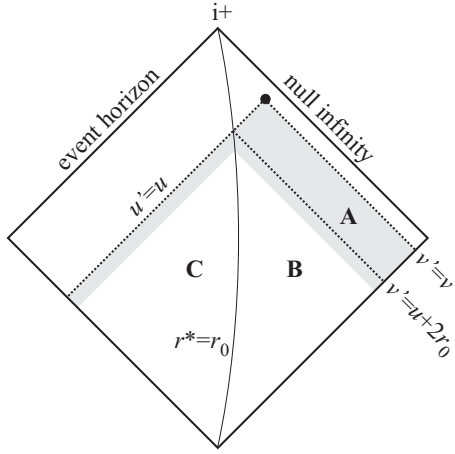


FIG. 7. Construction of the Green's function for a given external evaluation point at u, v . Regions where the Green's function is *not* exponentially small are indicated by dark color.

In region A ($u' \leq u, u+2r_0 \leq v' \leq v$) G is given by Eqs. (28) and (29), and is the same as in the shell model. In region B ($v' \leq u+2r_0, r_*' \geq r_0$) G is given by Eq. (34). It vanishes here exponentially towards early advanced time v' , and it possesses significant amplitude only within a narrow ingoing null “band” (of typical width $2r_0$), adjacent to region A. Then, in region C ($u' \leq u, r_*' \leq r_0$) the Green's function [given by Eq. (40)] vanishes exponentially towards early retarded time u' , and is of significant amplitude only within a narrow outgoing null “band” (of typical width $2r_0$) adjacent to the ray $u' = u$.

Like in the shell model, we find that the main region of effective sources covers only the range $u \leq v' \leq v$ of advanced times. In the shell model, however, the Green's function vanishes identically outside this range (due to the divergent potential at the center of symmetry), whereas in the complete SBH model it dies off exponentially (and also “penetrates” through the finite potential barrier at $u' = u$).

VI. CALCULATION OF Ψ_1 AT NULL INFINITY

We have shown that in the complete SBH model, Ψ_0 gives only an exponentially decaying contribution to the late time radiation. In this section we calculate the contribution of Ψ_1 to this radiation at null infinity, and show that it is characterized by the same power-law tail of decay that was indicated in the shell model. Moreover, we show that even the amplitudes of the waves are the same on both models, provided that we choose $|u_0| \gg 2M \simeq r_0$ (the difference is of order r_0/u_0).

Before we present the detailed calculation of Ψ_1 , we first give some heuristic arguments concerning the expected results. Figure 8 shows the region of spacetime in which scalar sources affect the behavior of the wave at null infinity, at a given retarded time $u \gg M$. Also shown, superposed, is the region where sources due to Ψ_0 exist. Outside the overlapping of these two areas, the

Green's function, or Ψ_0 , or both, are exponentially small. We expect (and later show analytically) that sources outside the overlapping area shall give only an exponentially decaying contribution to Ψ_1 at null infinity as $u \rightarrow \infty$. We may thus focus only on the two overlapping regions shown in the figure. One of these regions lies inside the surface $r_* = r_0$ (see the figure). It is of “dimensions” $r_0 \times r_0$, and is located near $r_* = (-u/2) \ll M$. In this location the potential function $V(r_*)$ is exponentially small (see figure 1), and thus the contribution from this area should be exponentially small as well. We are left with the contribution of sources at the “main” region [namely $u_0 \leq u' \leq 0, u \leq v' \leq v$], in which both the Green's function and Ψ_0 are having the same form as in the shell model, except for in a narrow band (of width $\sim 2r_0$) at the edge of this region. This suggests that for r_0 small enough, the calculation of Ψ_1 should yield a result very close to that obtained in the shell model.

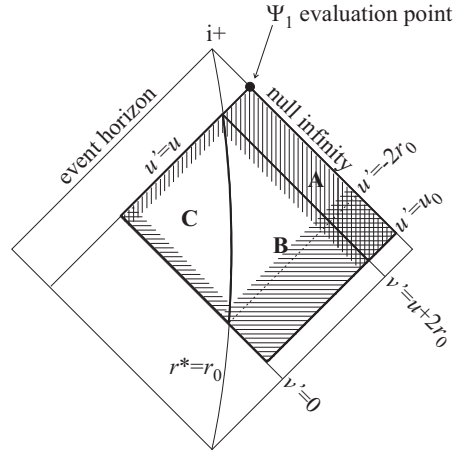


FIG. 8. calculation of Ψ_1 in the complete Schwarzschild model. The region filled with horizontal lines is where the amplitude of Ψ_0 is significant, while the region marked with vertical lines is where the Green's function is significant, in accordance with the discussion given in the text. Potentially, significant contribution to Ψ_1 is expected to arise only from areas where the two indicated regions overlap.

To confirm the above heuristic indications, we shall now calculate Ψ_1 at null infinity. In terms of the Green's function derived above, we formally have

$$\Psi_1^\infty(u) = - \int_{u_0}^u du' \int_0^v dv' G^\infty(u; u', v') \delta V(u', v') \Psi_0(u', v'), \quad (42)$$

where Ψ_1^∞ and G^∞ stand for the value of Ψ_1 and G at null infinity (that is, for $v \rightarrow \infty$). For the purpose of calculation, we separate the domain of integration into three regions,

$$\int_{u_0}^u du' \int_0^v dv' =$$

$$\int_{u+2r_0}^{\infty} dv' \int_{u_0}^u du' + \int_0^{u+2r_0} dv' \int_{u_0}^{v'-2r_0} du' + \int_0^{u+2r_0} dv' \int_{v'-2r_0}^u du' \quad (43)$$

to be labeled **A**, **B**, and **C**, respectively, as indicated in figure 8. In what follows we consider separately the contribution from each of these three regions to Ψ_1^{∞} . We show that the contribution of region **A** is the dominant one, and that this contribution is identical (in its pattern of late time decay, and also, to a certain order of accuracy, in its amplitude) to that obtained in the shell model.

Contribution from region C

In terms of the new integration variables $r'_* \equiv (v' - u')/2$ and $t' \equiv (v' + u')/2$, and using Eqs. (26) and (40) (with $r_* \rightarrow \infty$), the contribution to Ψ_1^{∞} from sources in region **C** takes the form

$$\begin{aligned} \Psi_{1C}^{\infty} = & -2r_0^{-l} \sum_{i,j=1}^{l+1} \alpha_j \gamma_{li} \int_{-u/2}^{r_0} dr'_* \int_{-r'_*}^{u+r'_*} dt' E_i(u - t' + r'_*) \\ & \times V(r'_*) E_j(t' + r'_* - 2r_0). \end{aligned} \quad (44)$$

(recall that in region **C**, where $r'_* < r_0$, we have $\delta V = V$ by definition.)

Since $V(r'_*) \propto \exp[(r'_*/2M)]$ for $r'_* \rightarrow -\infty$, one finds that the integrand in the last expression dies off exponentially in retarded time u anywhere inside the domain of integration. It is easy to verify that the integral itself would be exponentially small for large u/M . For example, for any fixed retarded time $u \gg M$ there exist positive constants c_1, c_2, c_3, c_4 and κ , such that the following upper bound is applicable to the above integral (in absolute value):

$$\begin{aligned} |\Psi_{1C}^{\infty}| \leq & \sum_{i,j=1}^{l+1} |\alpha_j \gamma_{li}| \left\{ c_1 \int_{-u/2}^{-u/4} dr'_* \int_{-r'_*}^{u+r'_*} dt' V(r'_*) \right. \\ & + c_2 \int_{-u/4}^{r_0} dr'_* \int_{-r'_*}^{\frac{u+r'_*}{2}} dt' |E_i(u - t' + r'_*)| \\ & \left. + c_3 \int_{-u/4}^{r_0} dr'_* \int_{\frac{u+r'_*}{2}}^{u+r'_*} dt' |E_j(t' + r'_* - 2r_0)| \right\} \\ \leq & c_4 \exp[-\kappa(u/r_0)]. \end{aligned} \quad (45)$$

We conclude that internal sources of Ψ_0 (namely sources at $r_* < r_0$) give at most an exponentially decaying contribution to the late time radiation at null infinity.

Contribution from region B

By Eqs. (13b) and (34) (with $r_* \rightarrow \infty$), the contribution from region **B** to Ψ_1 at null infinity reads

$$\begin{aligned} \Psi_{1B}^{\infty} = & \sum_{i=1}^{l+1} \sum_{n,j=0}^l \bar{\beta}_{nji} \int_0^{u+2r_0} dv' E_i(u - v' + 2r_0) \\ & \times \int_{u_0}^{v'-2r_0} du' \frac{(r'_* - r_0)^{l-j} r_0^j}{(r'_*)^{2l-n}} \delta V(r'_*) g_0^{(n)}(u'), \end{aligned} \quad (46)$$

in which $\bar{\beta}_{nji}$ are certain constant coefficients, and the function $g_0(u')$ stands for the expressions derived in the previous chapter for $g_0^I(u')$ and $g_0^{II}(u')$ [Eqs. (15) and (19), respectively]. If we now integrate this expression by parts with respect to v' , we find that *to the leading order in M/u and in r_0/u* ,

$$\begin{aligned} \Psi_{1B}^{\infty} = & \sum_{n=0}^l \sum_{j=0}^l \tilde{\beta}_{nj} r_0 \int_{u_0}^u du' \frac{(u - u')^{l-j} r_0^j}{(u - u' + 2r_0)^{2l-n}} \\ & \times \delta V(u - u' + 2r_0) g_0^{(n)}(u'), \end{aligned} \quad (47)$$

with $\tilde{\beta}_{nj}$ being some other coefficients. Now, integrate in parts each of the terms n successive times with respect to u' . The resulting surface terms would all be negligible at large u/r_0 , since $g_0(u')$ dies off exponentially at large retarded time u [see Eq. (19)]. In addition, these surface terms are strictly compact from below. We are left with

$$\begin{aligned} \Psi_{1B}^{\infty} = & \sum_{n=0}^l \sum_{j=0}^l (-1)^n \tilde{\beta}_{nj} r_0 \int_{u_0}^u du' g_0(u') \\ & \times \frac{d^n}{du'^n} \left[\frac{(u - u')^{l-j} r_0^j}{(u - u' + 2r_0)^{2l-n}} \delta V(u - u' + 2r_0) \right], \end{aligned} \quad (48)$$

to the leading order in M/u and in r_0/u .

To continue, we shall have to write δV in terms of the null coordinates. This cannot be done explicitly, since the function $r(r_*)$ is implicit. Rather, we shall use the large r expansion

$$\delta V(r_* \geq r_0) = Mr_*^{-3} [a + b \ln(r_*/2M)] + \mathcal{O}(M^2 r_*^{-4} [\ln(r_*/2M)]^2), \quad (49)$$

where a and b are constant coefficients, depending only on l and M . In paper I we argued that (in the framework of the shell model) it is merely the asymptotic form of the background potential which affects Ψ_1^{∞} at $u \gg M$. This has been also tested numerically (see figure 11 in paper I). We now proceed by assuming that the same is true in the complete SBH model as well.

With δV taken to the leading order in M/r_* , Eq. (48) takes the form

$$\begin{aligned} \Psi_{1B}^{\infty} = & Mr_0 \sum_{j=0}^l \sum_{m=0}^{l-j} \int_{u_0}^u du' g_0(u') \frac{(u - u')^{l-j-m} r_0^j}{(u - u' + 2r_0)^{2l-m+3}} \\ & \times \left[a_{jm} + b_{jm} \ln \left(\frac{u - u' + 2r_0}{2M} \right) \right], \end{aligned} \quad (50)$$

to the leading order in M/u and in r_0/u , where a_{jm} and b_{jm} are certain constant coefficients. We observe that,

since $g_0(u') \sim \exp(-u'/r_0)$ at large u' , the upper part of the integration over u' (say, between $u' = \sqrt{uM}$ and $u' = u$) gives a contribution which dies off exponentially at large u . In our approximation we can thus concentrate on the contribution coming from early retarded times (say, $u_0 \leq u' \leq \sqrt{uM}$). At any large enough retarded time u there exist positive constants c_5 and c_6 such that this early contribution (in absolute value) is bounded from above by

$$\begin{aligned} |\Psi_{1B}^\infty| &\leq c_5 M r_0 \sum_{j=0}^l \sum_{m=0}^{l-j} \frac{[(uM)^{1/2} - u_0](u - u_0)^{l-j-m} r_0^j}{[u - (uM)^{1/2} + 2r_0]^{2l-m+3}} \\ &\quad \times \left[|a_{jm}| + |b_{jm}| \ln \left(\frac{u - u_0 + 2r_0}{2M} \right) \right] \\ &\leq c_6 r_0 M u^{-(l+2.5)} \ln(u/M). \end{aligned} \quad (51)$$

In what follows it will become apparent that this contribution to the late time radiation at null infinity dies off more rapidly than the radiation due to scattering in the “main” region of sources (region **A**), which will be shown to be characterized by a u^{-l-2} decay tail. Therefore, the contribution from region **B** is negligible at $u \gg M$.

Contribution from region A (the “main” region)

The remaining contribution to calculate is that coming from region **A**, reading

$$\Psi_{1A}^\infty(u) = - \int_{u_0}^u du' \int_{u+2r_0}^\infty dv' G^\infty(u; u', v') \delta V(u', v') \Psi_0(u', v'). \quad (52)$$

To evaluate this expression we first write $\Psi_0(u', v')$ in terms of a function $g_0(u')$ [as in Eqs. (13a),(13b)], then integrate by parts each of the resulting terms in the r. h. s n successive times with respect to u' . Neglecting surface terms, which are all exponentially small at late time since $g_0 \sim \exp[-u/r_0]$ at large u , we obtain

$$\begin{aligned} \Psi_{1A}^\infty(u) &= - \sum_{n=0}^l (-1)^n A_n \int_{u_0}^u du' \int_{u+2r_0}^\infty dv' g_0(u') \\ &\quad \times \frac{\partial^n}{\partial u'^n} \left[\frac{G^\infty(u; u', v') \delta V(u', v')}{(v' - u')^{2l-n}} \right]. \end{aligned} \quad (53)$$

With the explicit form of the Green’s function [Eqs. (28) and (29)], and with δV taken to the leading order in M/r_* , the last equation takes the form

$$\begin{aligned} \Psi_{1A}^\infty(u) &= M \sum_{k=0}^l \sum_{j=0}^{l-k} \int_{u_0}^u du' \int_{u+2r_0}^\infty dv' \frac{(u - u')^{l-k-j} (v' - u)^k}{(v' - u')^{2l-j+3}} \\ &\quad \times \left[\bar{a}_{kj} + \bar{b}_{kj} \ln \left(\frac{v' - u'}{2M} \right) \right] g_0(u'). \end{aligned} \quad (54)$$

where \bar{a}_{kj} and \bar{b}_{kj} are certain constant coefficients that depend on l and M , but *not* on r_0 . Integrating over v' , the r. h. s of the last equation becomes

$$\begin{aligned} M \sum_{k=0}^l \sum_{j=0}^{l-k} \sum_{m=0}^k &\int_{u_0}^u du' \frac{(u - u')^{l-k-j} (r_0)^{k-m}}{(u - u' + 2r_0)^{2l-j-m+2}} \times \\ &\left[\tilde{a}_{kjm} + \tilde{b}_{kjm} \ln \left(\frac{u - u' + 2r_0}{2M} \right) \right] g_0(u'). \end{aligned} \quad (55)$$

with \tilde{a}_{kjm} and \tilde{b}_{kjm} being yet another constant coefficients, independent of r_0 .

Now, since $g_0(u')$ falls off exponentially at large u' , we may cut off the integration at, say, $u' = (Mu)^{1/2}$ without affecting the integral to the leading order in M/u . Doing so, we observe that the leading order contribution to this integral comes only from terms corresponding to $m = k$. (Note the way the dependence in the parameter r_0 cancels in the leading order).

Defining

$$\int_{u_0}^{\sqrt{uM}} g_{0I}(u) du' \simeq \int_{-\infty}^{\infty} g_{0I}(u) du' \equiv I_0, \quad (56)$$

(were the first equality holds to the leading order in M/u , as g_0 is compact from below and dies off exponentially at large u) we find that to the leading order in M/u , in r_0/u and in u_0/u ,

$$\Psi_1^\infty = M I_0 u^{-l-2} [k_1 + k_2 \ln u/M]. \quad (57)$$

k_1 and k_2 are constant coefficients that do *not* depend on r_0 . The only remaining reference to the value of r_0 lies within the integral I_0 .

Since the values of the coefficients k_l and k_2 are independent of r_0 , then in order to obtain these values one may use Eq. (52) with whatever value of this parameter (requiring only that $r_0 \ll u$). Now, if we take $r_0 = 0$, then Eq. (52) becomes completely analogous to the expression for Ψ_1^∞ in the shell model (Eq. (37) in paper I). Comparing these two expressions, we find that the Green’s function G and the potential δV appearing in both integrands are exactly the same. The two expressions differ only in the form of the function Ψ_0 , which on both cases is expressed in a similar way [as in Eq. (13a)] in terms of two different functions $g_0(u)$. However, the explicit form of the function $g_0(u)$ (as related to the initial data) has no effect whatsoever on the value of the coefficients k_l and k_2 and so these coefficients must be the same as in the shell model. Therefore, comparing Eq. (57) with Eq. (52) of paper I, we learn that $k_2 = 0$, and that, to the leading order in M/u , in u_0/u , and in r_0/u we have

$$\Psi_1^\infty(u \gg M) = 2(-1)^{l+1} (l+1)! M I_0 u^{-l-2}. \quad (58)$$

[for the compact initial data setup].

We conclude that the wave Ψ_1^∞ has the same late time behavior in the complete SBH model as it has in the

shell model, namely it dies off as u^{-l-2} provided that the initial pulse is compact. Numerical calculation of Ψ_1 in the complete SBH model agree with this result, as demonstrated in figure 9.

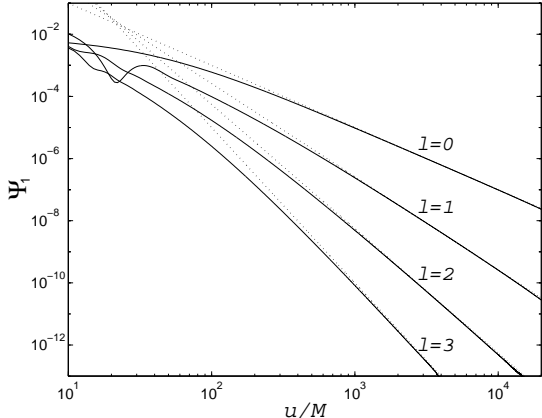


FIG. 9. Late time tails of Ψ_1 at null infinity. Presented on a log-log scale are numerical results obtained for Ψ_1 in the complete SBH model at $v = 10^5 M$ (approximating null-infinity), for the $l = 0, 1, 2, 3$ modes. (For $l = 0$ we used the definition of Ψ_1 given at the end of section VI). Compact initial data for the numerical propagation has been specified between $u = -40M$ and $u = -50M$, and the parameter r_0 has been set to $3M$. Also shown, for reference, are dotted lines proportional to u^{-l-2} . The results demonstrate the u^{-l-2} late time decay rate predicted by the analytic calculation.

We may similarly obtain the u^{-l-1} decay characterizing the static initial setup, by comparing Eq. (57) with Eq. (54) of paper I. If a static scalar field is present outside the central object up to some moment before the event horizon forms (no static solution exist which is well behaved both at the event horizon and at infinity), we shall have, to the leading order in M/u , in u_0/u , and in r_0/u ,

$$\Psi_1^\infty(u \gg M) = (-2)^{l+1} \frac{(l!)^2}{(2l)!} M \mu u^{-l-1}, \quad (59)$$

where μ represents the amplitude of the initial static field.

It is also instructive to compare the amplitudes of the wave Ψ_1^∞ at some fixed $u \gg M$ value on both models (the shell and the complete SBH), given the same initial data. As implied by the above discussion, the relative amplitude is simply given by the ratio of the integrals $I_0 \equiv \int_{u_0}^\infty g_0(u') du'$ associated with both models. Relying on the explicit expressions derived for the functions g_0 in this paper and in paper I, it can be easily shown that the two integrals I_0 , associated with the two models, differ merely by an amount of order $\sim r_0/u_0$. Thus, concentrating on the case $|u_0| \gg 2M \sim r_0$ (in the context of which our analysis proves effective—see the discussion in the following section), one observes no difference between the late time behavior of the wave Ψ_1 at null infinity on both models. This result is accurate to the leading order in M/u , in u_0/u and in r_0/u_0 . In particular, we may

conclude that at late time the wave Ψ_1^∞ has no reference (in our approximation) to the value of neither the radius of the shell R (in the shell model) nor the parameter r_0 (used in the complete SBH model). This result is consistent with the assumption that details of spacetime structure at small r values are not manifested in the form of the late time radiation.

The monopole case ($l = 0$)

It was pointed out while introducing the iterative expansion, that a scheme based on that expansion fails to handle correctly the case $l = 0$. In the monopole case it is straightforward to find that a Green's function defined as in sec. V is *constant* (a unity) throughout the whole range of evolution. It then follows that the wave Ψ_1 is constant at late time, resulting in the divergence of higher terms of the expansion (Ψ_2, Ψ_3, \dots) . Looking for the cause of this failure, we notice that in the cases $l > 0$ it is the centrifugal potential barrier that “cuts off” the Green's function and confines it (for late retarded time evaluation points, $u \gg M$) mainly to late retarded times ($u < u' < v$). In the shell model (see paper I) it was the presence of the center of symmetry which effectively acted as a potential barrier for the Green's function even in the monopole case, where no centrifugal potential exists. This is why the iterative expansion applied in the framework of the shell model proved to be equally effective for all modes of the radiation.

To analyze the case $l = 0$ in the complete SBH model, one is thus led to try a different iterative expansion, defined such that the Green's function is subject to an appropriate potential barrier, as for the modes with $l > 0$. One technically simple possibility it to take

$$V_0^{l=0} \equiv M^{-1} \delta(r_*). \quad (60)$$

We then define the iterative expansion as in Eqs. (10), (11), (12), with the ‘new’ potential $V_0^{l=0}$. With this definition, we find that $\Psi_0^{l=0} = \Gamma(u)$, and that the Green's function (at an evaluation point u, v with $(v - u)/2 = r_* > 0$) is given by

$$\begin{cases} G(u' \leq u, u \leq v' \leq v) = 1 \\ G(u' \leq v' \leq u) = \exp[(v' - u)/M] \\ G(v' \leq u' \leq u) = \exp[(u' - u)/M] \end{cases}. \quad (61)$$

(The three regions indicated in this equation are those labeled ‘A’, ‘B’, and ‘C’, respectively, in Fig. (7), when setting $r_0 = 0$). A simple calculation [based on Eq. (42)] then shows that at null infinity $\Psi_1^{l=0}$ is given by Eqs. (58) and (59) (with $l = 0$). These equations are therefore valid for all modes l .

VII. HIGHER TERMS OF THE ITERATIVE EXPANSION

The Green's function technique applied thus far provides a formal way to calculate each of the terms Ψ_N one at a time, in an inductive manner. We shall not, however, calculate further terms of the expansion, but rather we will refer to the results of the analysis in paper I. Regarding the shell model, strong indications were given that

- The dominant contribution to $\Psi_N^\infty (u \gg M)$, for all $N \geq 1$, is only due to sources of Ψ_{N-1} at large distances.
- All terms Ψ_N of the iterative expansion (excluding Ψ_0) seem to share the same late time pattern of decay at null infinity, namely a u^{-l-2} inverse power-law tail (for compact initial pulse), or a u^{-l-1} tail (for static initial field).
- If the initial pulse is confined to large distance, $|u_0| \gg M$, then the iterative sum converges at null infinity rather efficiently to the 'complete' scalar wave Ψ at late retarded time u .
- Moreover, in this case ($|u_0| \gg M$), the scalar wave Ψ is well approximated by merely Ψ_1 (with corrections smaller by order M/u_0).

Now, it is reasonable to assume that all four of the above results are also valid in the complete SBH model. For, in both models (the SBH and the shell models) spacetime structure at large distance is the same, and, as argued in paper I, it is the large distance region whose structure is relevant in determining the late time form of the waves at null-infinity. (This conclusion has been demonstrated in the framework of the shell model by explicit analytic calculation of Ψ_1 and Ψ_2 at null-infinity. Physical explanation was given in the concluding section of paper I. For the complete SBH model, a demonstration is provided by the explicit analytic calculation of Ψ_1^∞ in the preceding section). Actually, we need only to assume that the first of the four results indicated above holds in the complete SBH model. Then, the same reasoning used in section VII of paper I in deriving Eq. (72), leads us immediately to realize that $\Psi_N \sim u^{-l-2}$ in the SBH model as well. Also, a completely analogous analysis to that applied in section VIII of paper I shows that the third and forth of the above results hold in the complete SBH model as well.

Numerical analysis of the complete SBH model firmly supports the above arguments, showing that all four results are indeed valid in the complete SBH model. In what follows we present some examples of these numerical experiments.

Figure 10 presents the ratio $\Psi_1^\infty/\Psi^\infty$, calculated numerically for the monopole and the dipole modes, for various values of the parameter u_0 . (The "complete"

wave Ψ has been obtained by a direct numerical solution of Eq. (5)). The results demonstrate that (like in the shell model) as $|u_0|/M$ is set larger, Ψ_1 becomes a better approximation to the "complete" wave Ψ at null infinity at late time.

In figure 11 it is demonstrated numerically (for $l = 0, 1, 2$) that the iterative series applied in this paper seems to converge rather efficiently for a large $|u_0|/M$ value.

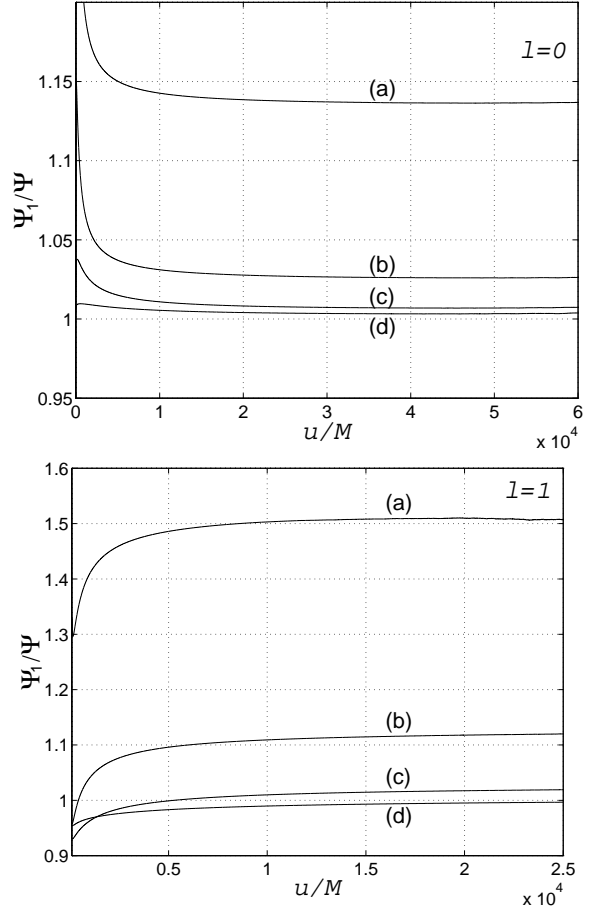


FIG. 10. Ψ_1 approximates the "complete" wave Ψ at null infinity at late time, provided that the parameter $|u_0|/M$ is chosen large. This is demonstrated numerically for the monopole ($l = 0$) and the dipole ($l = 1$) radiation by comparing the ratios Ψ_1/Ψ at null infinity (approximated by $v = 10^5 M$) for the various values (a) $u_0 = -40M$, (b) $u_0 = -200M$, (c) $u_0 = -1000M$, and (d) $u_0 = -5000M$. The parameter r_0 is set to $3M$.

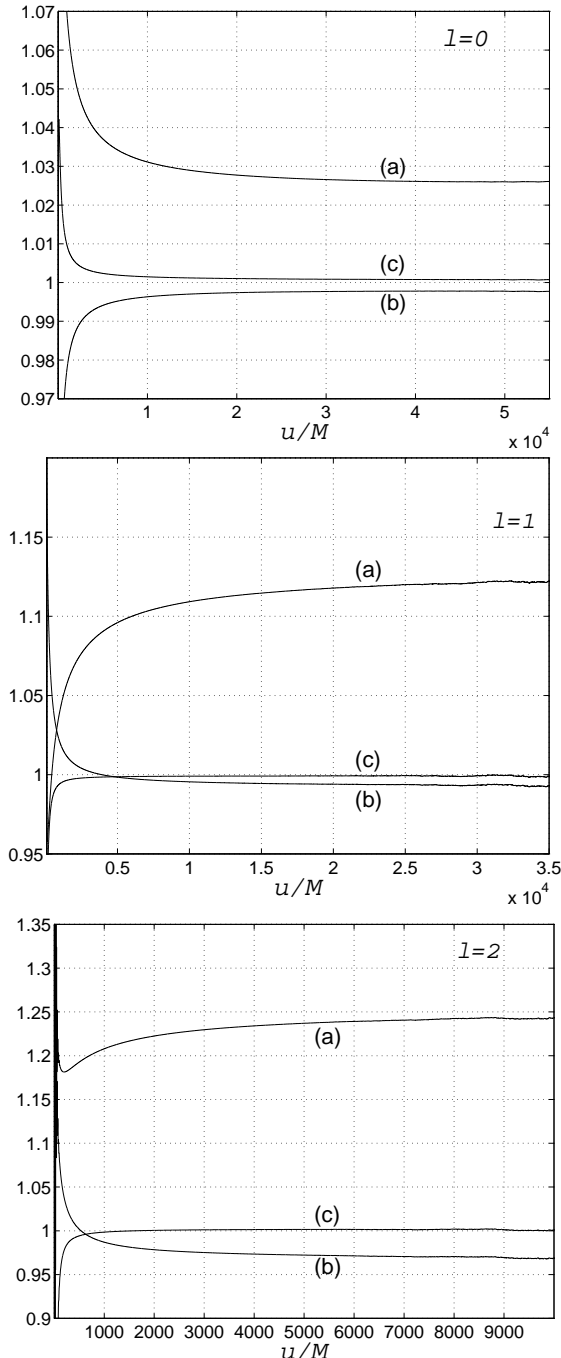


FIG. 11. Numerical indications for convergence of the iterative scheme at null infinity. Presented (on a linear scale) are the ratios (a) Ψ_1/Ψ , (b) $\frac{\Psi_1+\Psi_2}{\Psi}$, and (c) $\frac{\Psi_1+\Psi_2+\Psi_3}{\Psi}$ for the sample values $l = 0, 1, 2$. The other parameters are set to $r_0 = 3$, $u_0 = -200M$ and $v = 10^5M$ (approximating null infinity). The results suggest a rather efficient convergence of the iterative expansion for large $|u_0|/M$ values at large retarded time u .

VIII. TAILS AT CONSTANT RADIUS: THE LATE TIME EXPANSION

So far we were discussing an analytic technique enabling the calculation of the late time behavior of the scalar field at null infinity. In this section we apply a different, local, analysis to study the late time behavior of the wave along any $r = \text{const}$ world-line outside the black hole, and along the event horizon. Using this method we will be able to derive a simple analytic expression for the field, consistent with an inverse power-law decay, and accurate to the leading order in M/t (or in M/v along the horizon). However, this expression will inhere two undetermined parameters (one for the power-law index and the other for the amplitude). We shall deduce these parameters by matching our late time solution at null infinity to the form derived in the previous sections using the iterative scheme. In that respect, the iterative scheme shall prove to be an essential key for the construction of a complete late time description of the wave behavior anywhere outside the black hole. The purpose of this section is to introduce and apply the local method.

We make the assumption that at late time, the Klein–Gordon scalar wave [priorly separated in terms of the spherical harmonics as in Eq. (2)] admits the expansion

$$\phi^l(r, v) = \sum_{k=0}^{\infty} F_k^l(r) v^{-k_0 - k}, \quad (62)$$

in which the number k_0 and the set of functions $F_k(r)$ are yet to be determined. Substituting this expression in the Klein–Gordon equation (3) and collecting terms of common v -power, the partial equation is thereby converted to an infinite set of *ordinary* coupled equations for the unknown functions $F_k(r)$,

$$r^2 \left(1 - \frac{2M}{r}\right) F_k'' + 2(r - M) F_k' - l(l + 1) F_k = 2(k_0 + k - 1)(r^2 F_{k-1}' + r F_{k-1}) \quad (63)$$

(for $k \geq 0$), where a prime denotes differentiation with respect to r , and where we have set $F_{-1} \equiv 0$. This set of equations exhibit only a ‘weak’ coupling, in the sense that each of the functions F_k depends only on its preceding function F_{k-1} , with F_0 obeying a closed homogeneous equation. This hierarchy allows one to treat each of these equations one by one, in an iterative way. In this procedure, each of the functions F_k (with $k \geq 1$) satisfies a closed second-order inhomogeneous equation.

We proceed as follows: First, we show that there exists a solution ϕ^l of the form (62), which is regular anywhere outside the black hole, in particular at the event horizon and at null infinity. Then, with the aid of our previous results at null infinity, we deduce the late time behavior of the scalar waves as detected by a static observer at any constant radius. In particular, we obtain the late time form of the waves along the event horizon.

We define a new dimensionless radial coordinate

$$\rho \equiv \frac{r - M}{M}, \quad (64)$$

which varies monotonically from the event horizon ($\rho = 1$) up to space-like infinity ($\rho = \infty$). In terms of the new variable, Eq. (63) takes the form

$$(\rho^2 - 1)F_k'' + 2\rho F_k' - l(l + 1)F_k = D_k(\rho)[F_{k-1}], \quad (65)$$

in which a prime now denotes differentiation with respect to ρ , and where $D(\rho)$ is the differential operator

$$D_k(\rho) = 2M(k_0 + k - 1)(\rho + 1)[(\rho + 1)\partial_\rho + 1]. \quad (66)$$

(Note that $D_k(\rho)$ depends on k_0 , but is independent of l). For $k = 0$, the r. h. s of Eqs. (65) vanishes.

We would like to construct solutions F_k to Eqs. (65) such that ϕ would be regular both at the event horizon and at infinity. To allow ϕ to be regular at the horizon (where the v coordinate takes finite values), we require all functions $F_k(\rho)$ to be regular at $\rho = 1$ ^{**}. We will now show that such regular solutions $F_k(\rho)$ do exist^{††}.

We shall construct the functions F_k in an iterative way, starting with F_0 . For $k = 0$, Eq. (65) is homogeneous, and its general solution is given by $F_0^l = a_0 P_l(\rho) + b_0 Q_l(\rho)$, where a_0 and b_0 are arbitrary parameters, $P_l(\rho)$ is the Legendre polynomial of order l , and $Q_l(\rho)$ is the Legendre function of the second kind, of order l . The polynomials $P_l(\rho)$ are, of course, finite at the event horizon ($\rho = 1$) and divergent (as ρ^l) at $\rho \rightarrow \infty$. Conversely, The functions $Q_l(\rho)$ diverge at the event horizon and vanish (as ρ^{-l-1}) at $\rho \rightarrow \infty$. Regularity of F_0 at the event horizon therefore requires that $b = 0$, hence we obtain

$$F_0^l(\rho) = a_0 P_l(\rho). \quad (67)$$

Now consider Eq. (65) for a general function F_k (with $k \geq 1$). The general solutions to the inhomogeneous equations read

$$\begin{aligned} F_k^l(\rho) &= a_k P_l(\rho) + b_k Q_l(\rho) \\ &+ P_l(\rho) \int_1^\rho \frac{Q_l(\rho') D_k(\rho')[F_{k-1}(\rho')]}{(\rho'^2 - 1)W(\rho')} d\rho' \\ &- Q_l(\rho) \int_1^\rho \frac{P_l(\rho') D_k(\rho')[F_{k-1}(\rho')]}{(\rho'^2 - 1)W(\rho')} d\rho', \end{aligned} \quad (68)$$

^{**} Had we apply a $1/t$ expansion of ϕ instead of the $1/v$ expansion (62), all functions F_k had to diverge at the horizon (where $t = \infty$) to assure regularity of the scalar wave there. For that reason, the $1/v$ expansion seems more plausible from the technical point of view.

^{††}In Mathematical terminology, Eq. (65) possesses a “regular singular point” at $\rho = 1$ (the event horizon)—see, for example, [15]. For this case, standard mathematical theory tells that series solution for F_0 and for F_1 can always be constructed near $\rho = 1$. However, for $k \geq 2$ the source term in Eq. (65) appears to involve logarithmic functions, for which case standard theory gives no clear rules.

where a_k and b_k are arbitrary parameters, and

$$W \equiv P_l' Q_l - P_l Q_l' = (\rho^2 - 1)^{-1} \quad (69)$$

is the Wronskian. Using the relation

$$Q_l(\rho) = P_l(\rho) \int_\rho^\infty \frac{W(\rho')}{P_l^2(\rho')} d\rho' \quad (70)$$

and integrating Eq. (68) by parts, we can then obtain

$$\begin{aligned} F_k^l(\rho) &= a_k P_l(\rho) + b_k Q_l(\rho) + \\ &P_l(\rho) \int_1^\rho d\rho' \frac{W(\rho')}{P_l^2(\rho')} \int_1^{\rho'} d\rho'' P_l(\rho'') D_k(\rho'')[F_{k-1}(\rho'')]. \end{aligned} \quad (71)$$

We now show by mathematical induction that with $b_k = 0$ (for all k), the functions $F_k(\rho)$ are all *analytic* at the event horizon. The first function, F_0 , is analytic at $\rho = 1$ by Eq. (67). Now, following the inductive procedure, assume that F_{k-1} is analytic at $\rho = 1$ for some $k \geq 1$. Then, $D_k(\rho'')[F_{k-1}(\rho'')]$ is analytic at $\rho'' = 1$, hence the integrand of the ρ'' integration in Eq. (71) is analytic at that point. We thus find that the integral over ρ'' can be written in the form $(\rho' - 1)\bar{f}(\rho')$, where $\bar{f}(\rho)$ is some function which is analytic at the horizon (this can be shown by expanding the integrand in a Taylor series near $\rho'' = 1$, where it is analytic). Since the polynomials P_l have no real zeros in the range $\rho \geq 1$ [16], and W diverges as $(\rho' - 1)^{-1}$ at the horizon, we conclude that the whole integrand of the ρ' integration is analytic at $\rho' = 1$, and therefore that the integral over ρ' must be analytic as well. Hence the solutions F_k , defined in an inductive way by Eq. (71), with $b_k = 0$ for all $k \geq 1$, are all analytic at the horizon.

By this we have shown that the wave equation admits solutions ϕ of the form (62), which are analytic at the event horizon. The most general of these solutions contains an infinite number of free parameters, one for each power of $1/v$

We do not know yet the value of the power index k_0 , appearing in the expansion (62). To obtain this value we shall now evaluate ϕ at null infinity. By this mean we will be able to (i) show that the form of ϕ at null infinity is consistent with the results of our iterative analysis (in particular, that ϕ is regular there); and (ii) deduce the value of k_0 by comparing the results arising from the two independent schemes.

We start by showing, using mathematical induction, that the functions F_k all have the asymptotic form

$$F_k(\rho \rightarrow \infty) \sim a_0 c_k \rho^{l+k}, \quad (72)$$

in which c_k are certain constant coefficients, other than zero and yet to be determined. Here and henceforth, the form $f(x) \sim cx^n$ (where c is some constant) means that $\lim_{x \rightarrow \infty} [f(x)/x^n] = c$. It appears most convenient to

prove Eq. (72) by first showing that^{††}

$$\frac{dF_k}{d\rho}(\rho \rightarrow \infty) \sim a_0(l+k)c_k\rho^{l+k-1}. \quad (73)$$

Then, Eq. (72) is implied.

The form (73) obviously applies for F_0 [given in Eq. (67)], with

$$c_0 = \frac{(2l+1)!!}{l!(2l+1)}, \quad (74)$$

which is just the coefficient of ρ^l in the polynomial $P_l(\rho)$.

Following the inductive procedure, we now assume that Eq. (73) applies for some $k \geq 0$, and show that this leads to $dF_{k+1}/d\rho \sim (l+k+1)a_0c_{k+1}\rho^{l+k}$. Our assumption necessarily implies that $F_k \sim a_0c_k\rho^{l+k}$. Hence, by Eq. (66) we have

$$D_{k+1}F_k \sim 2Ma_0c_k(k_0+k)(l+k+1)\rho^{l+k+1}. \quad (75)$$

Consequently, for the integration over ρ'' in Eq. (71) we obtain the asymptotic form

$$\sim 2Ma_0c_kc_0 \frac{(k_0+k)(l+k+1)}{(2l+k+2)}(\rho')^{2l+k+2}. \quad (76)$$

It then follows from Eq. (71) that

$$F_{k+1} \sim a_0c_{k+1}\rho^{l+k+1}, \quad (77)$$

with

$$c_{k+1} = 2Mc_k \frac{(k_0+k)(l+k+1)}{(2l+k+2)(k+1)}. \quad (78)$$

Finally, differentiating Eq. (77), we get $dF_{k+1}/d\rho \sim (l+k+1)a_0c_{k+1}\rho^{l+k}$, which establishes the inductive proof of Eq. (73).

We have thereby shown that the functions F_k all admit the asymptotic form (72), with the coefficients c_k given by the recursive formula (78), supplemented by Eq. (74). We obtain, in conclusion,

$$F_k \sim a_0\alpha_l(2)^k C_k M^{-l} r_*^{l+k} \quad (79)$$

for $r_* \rightarrow \infty$, where we have explicitly used the fact that $\rho \sim r/M \sim r_*/M$, and where

$$C_k = \frac{(k_0+k-1)!(l+k)!}{(2l+k+1)!(k)!}, \quad (80)$$

and

^{††}This is not valid when $l = 0$ and $k = 0$, for which case $dF_k/d\rho = 0$. However, the rest of the analysis does not change.

$$\alpha_l = \frac{(2l)!(2l+1)!!}{(l!)^2(k_0-1)!}. \quad (81)$$

(The coefficients C_k and α_l are not to be confused with the coefficients appearing in sec. (IV)).

Eq. (79) describes the form of the functions F_k to the leading order in r/M , which is sufficient for our purpose: matching ϕ at null infinity. We comment, however, that a full series expression for the functions F_k at large r can be obtained as well. It has the form

$$F_k(r) = r^k \sum_{j=0}^k (r/M)^{l-j} H_{kj}(M/r)[\ln(r/M)]^j, \quad (82)$$

where $H_{kj}(M/r)$ are Taylor series. This form can be verified by substituting it into Eq. (63), then constructing explicit recursive formulae for the coefficients of each of the various series H_{kj} . Note that to the leading order in r/M no logarithmic terms are involved, and the form (79) is recovered.

To obtain ϕ at null infinity, we insert Eq. (79) into the expansion (62). We get (to the leading order in r/M),

$$\phi = a_0\alpha_l(2M)^{-l}v^{l-k_0} \sum_{k=0}^{\infty} C_k \left(1 - \frac{u}{v}\right)^{l+k}. \quad (83)$$

To evaluate the power series, we write it in terms of a generating function,

$$\sum_{k=0}^{\infty} C_k q^k = q^{-2l-1} \frac{d^{k_0-2l-2}}{dq^{k_0-2l-2}} \left[q^{k_0-1} \frac{d^l}{dq^l} \left(\frac{q^l}{1-q} \right) \right], \quad (84)$$

which is valid for $|q| < 1$. In this expression the derivatives might be of negative orders, in which case integrations are implied. If we now make the substitution $q = (1 - \frac{u}{v})$, keeping just the leading order in u/v , we find that

$$\sum_{k=0}^{\infty} C_k \left(1 - \frac{u}{v}\right)^k = \frac{d^{k_0-l-2}}{dq^{k_0-l-2}} \left(\frac{1}{1-q} \right) = (k_0-l-2)! \left(\frac{v}{u} \right)^{k_0-l-1}. \quad (85)$$

Since $\Psi \equiv r\phi = v\phi$ to the leading order in u/v , we finally obtain

$$\Psi^\infty(u) = a_0\alpha_l(k_0-l-2)!(2M)^{-l}u^{-(k_0-l-1)}, \quad (86)$$

where $\Psi^\infty(u)$ stands for the wave Ψ evaluated at null infinity.

The value of both the power index k_0 and the yet-free parameter a_0 can now be specified by comparing the last result to the results arising from our iterative scheme, Eqs. (58) and (59). This comparison yields (assuming that $|u_0| \gg M$),

$$k_0 = \begin{cases} 2l+3 & \text{no initial static field} \\ 2l+2 & \text{initial static field} \end{cases}, \quad (87)$$

and

$$a_0 = \begin{cases} \frac{(l!)^2(2l+2)!}{(2l)!(2l+1)!!} (-2M)^{l+1} I_0 & \text{no initial static field.} \\ \frac{(l!)^3(2l+1)}{2(2l)!(2l+1)!!} (-4M)^{l+1} \mu & \text{initial static field} \end{cases}, \quad (88)$$

where the integral I_0 [defined in Eq. (56)] is directly related to the initial data via Eq. (15), and μ is the amplitude of the initial static field (when present).

Provided with an exact expression for $F_0(r)$ and with the value of k_0 , we are now in a position to write the form of the scalar field at any finite value of r , at very late time. By Eq. (62) we have, *to the leading order in M/t and in M/u_0 ,*

$$\Psi = \frac{a_0}{t^{2l+2,3}} r P_l \left(\frac{r-M}{M} \right), \quad (t \gg |r_*|); \quad (89)$$

and *to the leading order in M/v and in M/u_0 ,*

$$\Psi = \frac{2Ma_0}{v^{2l+2,3}}, \quad \text{at the event horizon,} \quad (90)$$

where the two values of powers correspond to the cases where an initial static field is or is not present, respectively.

We should emphasize here that the above results [Eqs. (89) and (90)] apply towards time-like infinity at *any* value of r , establishing [together with the results at null infinity, Eqs. (58), (59)] a *complete* picture of the late time behavior outside the black hole. To the best of our knowledge, such a result has never been obtained previously. (For example, in [1], [2], and [4], analytic expressions were derived only for the asymptotic domains $r_* \gg M$ and $r_* \ll M$.)

IX. CONCLUDING REMARKS

In this paper, and in the paper preceding it, we have tested the applicability of a new analytic scheme for the calculation of the late time behavior of fields outside black holes. It was demonstrated, considering the simple model of scalar waves outside a SBH, that a simple expansion of the field near time-like infinity can be used in order to construct a late time solution consistent with a power-law decay anywhere outside the black hole. However, the actual index of the power-law, as well as the amplitude coefficient of the wave (as related to the initial data) could not be determined merely by this local analysis. This information could be obtained only by a full integration of the 2-dimensional initial value problem for the wave evolution, technically enabled by the introduction and application of the iterative procedure.

Thus, by applying both the iterative scheme and the late time expansion, we were able to obtain an analytic expression for the scalar field in Schwarzschild, accurate to the leading order in M/t (or in M/u at null infinity,

or in M/v at the event horizon) and holding anywhere outside the black hole. The expression calculated is explicitly related [via Eqs. (15), (56), and (88)] to the form of arbitrary initial data specified at large distance (our approximate solution has corrections of order M/u_0).

Of course, the main justification for the introduction of the new approach should rely on its applicability to more realistic models of wave evolution, for which no other analytic approaches have been proposed. In what follows we mention some possible applications of our calculation scheme, which include the analysis of scalar fields outside Kerr black holes, the analysis of gravitational perturbations in Kerr, and the extension of our analysis to the interior of black holes.

The most interesting application of the new scheme concerns rotating black holes. As already mentioned in the introduction, this generalization is the prime motivation behind the presentation of our approach, since realistic stellar objects (and black holes) generically possess angular momentum. The generalization of our analysis to the case of scalar waves propagating in the exterior of a Kerr black hole shall be presented in a forthcoming paper. In brief, the basic idea behind this generalization is to express the lack of spherical symmetry in Kerr spacetime in terms of *interactions* between the various modes of spherical harmonics. The resulting interaction terms coupling the field equations for the various modes (these terms are expected to be small, in a sense, at late time) are then to be treated using our iterative technique. Applying an iterative decomposition basically similar to that used in the spherically-symmetric models, those interaction terms become source terms in the resulting hierarchy of wave equations. The mathematical treatment of these equations is then similar, in principle, to that applied in the spherically-symmetric cases. This provides the late time form of each of the modes at null infinity. Then, a generalization of the late time expansion method (based on the same interaction-between-modes approach) provides the late time behavior of the field anywhere outside the Kerr black hole, in particular along its event horizon. The details of both parts of the analysis in Kerr shall be given in [12] (see also [13]).

Obviously, the scalar model discussed so far is just a simplified analogue to the physical problem concerning the dynamics of gravitational perturbations. The plausibility of the scalar model stems from the remarkable resemblance of the underlying mathematical formulation, between this model and realistic models of gravitational waves (as was already realized in [1], for example, for the SBH case). Equations governing metric perturbations of the SBH were derived by Regge and Wheeler [17] (for axial perturbations) and by Zerilli [18] (for polar perturbations). Both equations can be put in the same form as the scalar field equation (5), where this time the wave function represents certain linear combinations of entities characterizing the metric perturbation. In both Regge-Wheeler's and Zerilli's equations one also finds that the effective potential is similar in shape to that of the scalar

model (Eq.(6) and figure 1). This suggests that the problem of gravitational waves propagation in the SBH geometry may be treated using the same iterative scheme applied for the scalar model.

We do not have similar separable equations for metric perturbations of Kerr black holes. Rather, a second approach, based on the Newman–Penrose tetrad formalism, was used by Teukolsky [19] to derive separable wave equations governing perturbations of the Weyl scalars. [An exhaustive discussion of field equations for gravitational perturbations is given in [20], pp. 174–182 (for Schwarzschild) and pp. 430–443 (for Kerr)]. Separation of Teukolsky’s equation is only possible in the frequency domain (namely by first separating the wave to its Fourier modes). To apply our iterative approach, however, the time dependence should rather be kept in the master Teukolsky equation. Instead, the master perturbation equation is to be treated in the way outlined above, namely, by considering interactions between the various modes of spherical harmonics. By now we have first indications that this approach is indeed applicable to gravitational perturbations (in the tetrad formalism). We intend to study this subject more deeply in the near future.

Finally, we mention the possibility of extending our analysis to internal perturbations of black holes. Recently, Ori used the technique of *late time expansion* (basically similar to the method presented in sec. VIII of the present paper), to explore the late time behavior of scalar fields *inside* charged [21] and rotating [22] black holes. In this analysis, boundary conditions for the wave evolution were assumed on the event horizon (in the form of an inverse power-law in v), and the asymptotic late time ($t \gg M$) behavior of the wave was deduced inside the black hole, up to the inner horizon. This provided a tool for exploring the nature of the inner horizon singularity. With the results of the external analysis (generalized to charged and rotating black holes), a connection may be established between the form of the wave at the inner horizon to its form at null infinity, which, in turn, using the iterative scheme, can be derived as explicitly related to the form of arbitrary initial data outside the black hole. That would allow one, given initial data outside the black hole (at large distance), to deduce the late time form of the wave at the inner horizon (including its accurate amplitude coefficient) without any assertion about the boundary conditions.

One may also think of a more rigorous and coherent scheme, which includes the simultaneous analysis of both internal and external perturbations, in the framework of a generalized late time expansion. This generalization becomes natural when applying an expansion of the form (62), as the coordinates v and r are both regular through the event horizon. Then a full treatment of both internal and external evolution is possible by following basically the same steps as described in sec. VIII, this time allowing the r coordinate to take its full range of values.

ACKNOWLEDGMENTS

The author wishes to express his indebtedness to Professor A. Ori for his guidance throughout the execution of this research and for countless helpful discussions.

* E. mail: leor@techunix.technion.ac.il

- [1] R. H. Price, Phys. Rev. D **5**, 2419 (1972); **5**, 2439 (1972).
- [2] C. Gundlach, R. H. Price, and J. Pullin, Phys. Rev. D **49**, 883 (1994).
- [3] R. Gómez, J. Winicour, and B. G. Schmidt, Phys. Rev. D **49**, 2828 (1994).
- [4] E. Leaver, J. Math. Phys. (N.Y.) **27**, 1238 (1986); Phys. Rev. D **34**, 384 (1986).
- [5] N. Andersson, Phys. Rev. D **55**, 468 (1997).
- [6] E. S. C. Ching, P. T. Leung, W. M. Suen, and K. Young, Phys. Rev. Lett. **74**, 2414 (1995).
- [7] L. M. Burko, A. Ori, Phys. Rev. D **56**, 7820 (1997).
- [8] C. Gundlach, R. H. Price, and J. Pullin, Phys. Rev. D **49**, 890 (1994).
- [9] P. R. Brady, C. M. Chambers, W. Krivan, and P. Laguna, Phys. Rev. D **55**, 7538 (1997).
- [10] W. Krivan, P. Laguna, and P. Papadopoulos, Phys. Rev. D **54**, 4728 (1996).
- [11] W. Krivan, P. Laguna, P. Papadopoulos, and N. Andersson, Phys. Rev. D **56**, 3395 (1997).
- [12] L. Barack, A. Ori, *Late time tails in Kerr geometry*, in preparation.
- [13] L. Barack in *Internal structure of black holes and space-time singularities*, Volume XIII of the Israel Physical Society, Edited by L. M. Burko and A. Ori, (Institute of Physics, Bristol, 1997).
- [14] F. G. Friedlander, *The wave equation on a curved space-time* (Cambridge University Press, Cambridge, 1975), section 5.4 (see in particular theorems 5.4.1 and 5.4.2).
- [15] H. Wayland, *Differential equations applied in science and engineering* (D. Van Nostrand Company, Princeton, New Jersey, 1957), pp. 131–146.
- [16] I. S. Gradshteyn, I. M. Ryzhik, *Tables of integrals, series and products*, §8.782.
- [17] T. Regge and J. A. Wheeler, Phys. Rev. **108**, 1063 (1957).
- [18] F. J. Zerilli, Phys. Rev. D **2**, 2141 (1970).
- [19] S. A. Teukolsky, Phys. Rev. Lett. **29**, 1114 (1972).
- [20] S. Chandrasekhar, *The Mathematical Theory of Black Holes* (Oxford University Press, New York, 1983).
- [21] A. Ori, Phys. Rev. D **55**, 4860 (1997)
- [22] A. Ori, Phys. Rev. D, in press.